Supplemental Information to "Bacterial immunogenic α-galactosylceramide identified in the murine large intestine: dependency on diet and inflammation"

Authors

Johanna von Gerichten[1,2], Dominic Lamprecht[1], Lukáš Opálka[1,3], Daphnée Soulard[4], Christian Marsching[5], Robert Pilz[1,2], Valentin Sencio[4], Silke Herzer[6], Bruno Galy[7], Viola Nordström[6], Carsten Hopf[5], Hermann-Josef Gröne[6,8], François Trottein[4], Roger Sandhoff[1,*]

Affiliations

[1] Lipid Pathobiochemistry Group, Department of Cellular and Molecular Pathology, German Cancer Research Center, Heidelberg, Germany[2] Faculty of Biosciences, University of Heidelberg

[3] Skin Barrier Research Group, Department of Organic and Bioorganic Chemistry, Faculty of Pharmacy in Hradec Králové, Charles University

[4] Centre d'Infection et d'Immunité de Lille, Inserm U1019, CNRS UMR 8204, University of Lille, CHU Lille, Institut Pasteur de Lille, 59000 Lille, France

[5] Center for Mass Spectrometry and Optical Spectroscopy (CeMOS), Mannheim University of Applied Sciences, Mannheim, Germany

[6] Department of Cellular and Molecular Pathology, German Cancer Research Center, Heidelberg, Germany

[7] Division of virus-associated carcinogenesis, German Cancer Research Center, Heidelberg, Germany

[8] Institute of Pharmacology, University of Marburg, Marburg, Germany.

***Correspondence**: Roger Sandhoff, DKFZ-Heidelberg (G131), INF 280, D-69120 Heidelberg, Germany, Tel. +49-6221-424358, Email: r.sandhoff@dkfz.de

Running title: Bacterial α-GalCer found in mouse large intestine

Supplemental Methods

Synthesis of αGalCer(d18:1/βh16:0), βGalCer(d18:1/βh16:0), and αGlcCer(d18:1/βh16:0) standards:

2.0 mg (4.3 µmol) of C18-α-, C18-β-galactosylsphingosine, or C18-α-glucosylsphingosine, 1.42 mg (5.2 µmol) of racemic 3-hydroxypalmitic acid and 2.0 mg (14.8 µmol) of 1-hydroxybenzotriazole were placed into a dry Schlenk tube and evacuated. The tube was filled with nitrogen and subsequently, 500 µL of dry tetrahydrofuran and 1.55 µL (8.8 µmol) of N-(3-dimethylaminopropyl)-N'-ethylcarbodiimide (EDC / WSC) were added. Compounds were dissolved with the rotating stirring bar and reaction carried on for 24 hours at room temperature under nitrogen atmosphere. Completion of reaction was determined by thin layer chromatography. Solutions were dried under a nitrogen stream. The crude products were purified by silica gel column chromatography ($CHCl_3$:CH_3OH:2.5M NH_4OH 6:4:1) to yield 0.9 mg (58%) of the final compound.

Synthesis of αGalCer(d18:0/βh16:0), βGalCer(d18:0/βh16:0), and αGlcCer(d18:0/βh16:0) standards:

Half of the reaction products of αGalCer(d18:1/βh16:0), βGalCer(d18:1/βh16:0), and αGlcCer(d18:1/βh16:0) standards (approximately 0.45 mg) were dried with a magnetic stirring bar in a Schlenk tube, dissolved in 2 mL of methanol:water (95:5) and a catalytic amount of 10% palladium on charcoal was added. The tube was flushed with nitrogen and subsequently nitrogen gas was exchanged for hydrogen gas (balloon technique). Reaction was carried on for 24 hours at room temperature and completion was determined by thin layer chromatography and by mass spectrometry. Reaction mixtures were filtered from palladium on charcoal and dried to obtain almost quantitative yield. The products were used without further purification.

Quantification of αGalCer(d18:1/βh16:0), βGalCer(d18:1/βh16:0), αGlcCer(d18:1/βh16:0), αGalCer(d18:0/βh16:0), βGalCer(d18:0/βh16:0), and αGlcCer(d18:0/βh16:0) standards:

The amount of synthesized α-, βGalCers, and αGlcCers was determined by anthrone reaction using a calibration solution of galactose or glucose with defined concentration according to a previous publication {Sandhoff, 2002 #830}.

Enrichment of Hexosylceramides containing GalCer(d18:0;h16:0) from a larger amount of mouse caeca:

We collected 79g wet weight of caeca from mice and distributed them into ten 50mL-polypropylene tubes. To each tube, 15 mL ice-cold methanol were added, and tissues were homogenized with an ULTRA TURRAX T25 basic on ice. Subsequently 15 mL chloroform were added to each tube. Homogenates were incubated with ultrasound for 15 min at 37 °C and subsequently centrifuged with 2000 g for 10 min. Supernatants were collected in a 2L-round bottom flask. Pellets were re-extracted with 30 mL chloroform:methanol:water (10:10:1) and finally with chloroform:methanol:water (30:60:8) as described above. Supernatants of each extraction step were collected with the first in the 2L-round bottom flask and concentrated to dryness with a rotary evaporator. The extract was taken up in 20 mL of 1 M KOH in methanol and incubated for 4 hours at 50 °C to hydrolyze glycerolipids. The reaction was stopped by addition of 1.15 mL concentrated acetic acid and salts were removed by dialysis (4 x 5L water over 36 hours). Content of the dialysis tube was washed out with methanol and dried first with a rotary evaporator and finally by freeze drying. Subsequently neutral and acidic compounds were separated by anion exchange column (13g dry DEAE Sephadex –A25) as described previously {Sandhoff, 2002 #830}. Neutral lipids including the GalCer(d18:0;h16:0) were collected in the flow through, desalted with RP18 cartridges, dried, taken up in 15 mL chloroform:methanol:water (10:10:1) and stored at -20 °C.

Lipid extraction from small amounts of mouse tissue:

Mouse tissue was homogenized in methanol on ice using the Quiagen TissueLyser II. One stainless steel bead (5 mm) per tube was agitated for 2 minutes at 25 Hz and homogenates were dried with a SpeedVac. Dried tissue samples were extracted 3 times for 15 min in an ultra sound bath with mixtures of chloroform/methanol/water (2x with 10/10/1 and then with 30/60/8). Supernatants were pooled, dried and subjected to methanolic mild alkaline hydrolysis (0.1 M potassium hydroxide) for 2 h at 37°C to eliminate glycerolipids and subsequently were neutralized with acetic acid. Saponified extracts were then desalted using reverse phase C-18 columns.

Lipid extraction from bacteria:

Dried bacteria samples were homogenized in methanol using the Quiagen TissueLyser II. One stainless steel bead (5 mm) per tube was agitated for 2 minutes at 25 Hz. Lysates were extracted in 1 mL chloroform/methanol (2/1) at 37°C for 15 min with occasional sonication. Lipid-containing supernatants were collected following centrifugation at 2000g for 10 min and pellets were then re-extracted once with chloroform/methanol/water (10/10/1) and once more with chloroform/methanol/water (30/60/8). Supernatants were pooled and dried.

Supplemental Tables

Supplemental Table S1: UPLC-gradient used to elute hexosylceramides from CSH C18 column.

Time [min]	Flow rate [mL/min]	Solvent A [%][a]	Solvent B [%][a]
Initial	0.35	57	43
0.2	0.35	57	43
0.4	0.35	50	50
4.0	0.35	30	70
10.0	0.35	5	95
11.0	0.35	5	95
11.5	0.35	1	99
12.0	0.35	57	43
13.0[b]	0.35	57	43

a) Solvent % are v/v. Solvent A: 50% methanol, 50% water, Solvent B: 1% methanol, 99% 2-propanol. Both solvents were supplemented either with 10 mM ammonium acetate and 10 nM EDTA (disodium salt) or with 0.1% formic acid, 10 mM ammonium formate and 5 µM citric acid .

b) After 13 min, the next sample was immediately injected. Besides the indicated gradient, there was no pre- or postwashing/equilibration steps between samples. However, before injection of biological samples a blank sample was introduced to ensure no contamination from standards.

Supplemental Table S2: UPLC-gradient used to elute hexosylceramides from CORTECS HILIC column.

Time [min]	Flow rate [mL/min]	Solvent A [%][a]	Solvent B [%][a]
Initial	0.3	100	0
0.75	0.3	100	0
4.50	0.3	56	44
5.50	0.3	0	100
6.50	0.3	0	100
8.00	0.3	100	0
25.00[b]	0.3	100	0

a) Solvent % are v/v. Solvent A: 97% propionitrile, 2% 2-butanol, 0.1% formic acid and Solvent B: 97% methanol, 2% 2-butanol, 0.1% formic acid, 10 mM ammonium formate

b) After 25 min, the next sample was immediately injected. Besides the indicated gradient, there was no pre- or postwashing/equilibration steps between samples. However, before injection of biological samples a blank sample was introduced to ensure no contamination from standards.

*Supplemental Table S3: Tandem-mass spectrometry transitions and collision energies used to **quantify** lipids in MRM mode.*

Compound	Precursor ion [m/z]	Product ion [m/z]	Collision energy [eV]
HexCer(d18:1/X:Y)	$[M+H-H_2O]^+$	$[So+H-2H_2O]^{+a}$	44
	$[M+H]^+$		
HexCer(d18:1/14:0)	654.53	264.27	
	672.54		
HexCer(d18:1/16:0)	682.56		
	700.57		
HexCer(d18:1/18:0)	710.59		
	728.60		
HexCer(d18:1/19:0)	724.61		
	742.62		
HexCer(d18:1/20:0)	738.62		
	756.64		
HexCer(d18:1/22:0)	766.66		
	784.67		
HexCer(d18:1/23:0)	780.67		
	798.68		
HexCer(d18:1/24:1)	792.67		
	810.68		
HexCer(d18:1/24:0)	794.69		
	812.70		
HexCer(d18:1/25:0)	808.70		
	826.71		
HexCer(d18:1/26:0)	822.72		
	840.73		
HexCer(d18:1/31:0)	892.80		
	910.81		
HexCer(dX:0/Y:Z)	$[M+H]^+$	$[Sa+H-H_2O]^{+b}$	44
HexCer(d17:0/15:0)	674.56	270.27	
HexCer(d17:0/16:0)	688.57		

HexCer(d18:0/14:0)	674.56	284.30	
HexCer(d18:0/15:0)	688.57		
HexCer(d18:0/16:0)	702.59		
HexCer(d18:0/18:0)	730.62		
HexCer(d18:0/19:0)	744.64		
HexCer(d18:0/20:0)	758.65		
HexCer(d18:0/21:0)	772.67		
HexCer(d18:0/22:0)	786.68		
HexCer(d18:0/23:0)	800.70		
HexCer(d18:0/24:1)	812.70		
HexCer(d18:0/24:0)	814.71		
HexCer(d18:0/25:0)	828.73		
HexCer(d18:0/26:0)	842.74		
HexCer(d19:0/15:0)	702.59	298.30	
HexCer(d19:0/16:0)	716.60		
Compound	**Precursor ion [m/z]**	**Product ion [m/z]**	**Collision energy [eV]**
HexCer(d18:1/hX:Y)	$[M+H-H_2O]^+$	$[So+H-2H_2O]^+$	44
	$[M+H]^+$		
HexCer(d18:1/h16:0)	698.56	264.27	
	716.57		
HexCer(d18:1/h18:0)	726.59		
	744.60		
HexCer(d18:1/h20:0)	754.62		
	772.63		
HexCer(d18:1/h22:0)	782.65		
	800.66		
HexCer(d18:1/h23:0)	796.67		
	814.68		
HexCer(d18:1/h24:1)	808.67		
	826.68		
HexCer(d18:1/h24:0)	810.68		
	828.69		
HexCer(d18:1/h25:0)	824.70		

	842.71		
HexCer(d18:1/h26:0)	838.71		
	856.72		
HexCer(dX:0/hY:Z)	$[M+H]^+$	$[Sa+H-H_2O]^+$	45
HexCer(d17:0/h16:0)	704.57	270.27	
HexCer(d17:0/h17:0)	718.62		
HexCer(d18:0/h16:0)	718.58	284.30	
HexCer(d18:0/h17:0)	732.60		
HexCer(d18:0/h18:0)	746.61		
HexCer(d18:0/h20:0)	774.65		
HexCer(d18:0/h22:0)	802.68		
HexCer(d18:0/h24:1)	828.69		
HexCer(d18:0/h24:0)	830.71		
HexCer(d19:0/h16:0)	732.60	298.30	
HexCer(d19:0/h17:0)	746.61		
HexCer(t18:0/X:Y)	$[M+H]^+$	$[So+H-H_2O]^+$	45
HexCer(t18:0/16:0)	718.58	282.30	
HexCer(t18:0/18:0)	746.61		
HexCer(t18:0/20:0)	774.65		
HexCer(t18:0/22:0)	802.68		
HexCer(t18:0/23:0)	816.69		
HexCer(t18:0/24:1)	828.69		
HexCer(t18:0/24:0)	830.71		
HexCer(t18:0/25:0)	844.72		
HexCer(t18:0/26:0)	858.74		
Compound	**Precursor ion [m/z]**	**Product ion [m/z]**	**Collision energy [eV]**
HexCer(t18:0/hX:Y)	$[M+H]^+$	$[So+H-H_2O]^+$	46
HexCer(t18:0/h16:0)	734.58	282.30	
HexCer(t18:0/h18:0)	762.61		
HexCer(t18:0/h20:0)	790.64		
HexCer(t18:0/h22:0)	818.67		
HexCer(t18:0/h23:0)	832.69		
HexCer(t18:0/h24:1)	844.69		

HexCer(t18:0/h24:0)	846.70		
HexCer(t18:0/h25:0)	860.72		
HexCer(t18:0/h26:0)	874.73		

a) So: sphingosine; b) Sa: sphinganine

*Supplemental Table S4: Tandem-mass spectrometry transitions and collision energies used to **identify** lipids in MRM mode.*

Compound	Precursor ion [m/z]	Product ion [m/z]	Collision energy [eV]
HexCer(dX:Y/hZ:0)	$[M+Na]^+$	Fragment **a** $[M+Na - H_2O]^+$	45
HexCer(d18:1/16:0)	722.56	704.55	
HexCer(d18:0/16:0)	724.57	706.56	
HexCer(d18:1/h16:0)	738.56	720.55	
HexCer(d17:0/h17:0)	740.57	722.56	
HexCer(d18:0/h16:0)			
HexCer(d18:0/h17:0)	754.59	736.58	
HexCer(d18:1/h18:0)	766.59	748.58	
HexCer(d19:0/h17:0)	768.60	750.59	
HexCer(dX:Y/hZ:0)	$[M+Na]^+$	Fragment **b** $[M+Na - C_6H_{10}O_5]^+$	45
HexCer(d18:1/16:0)	722.56	560.51	
HexCer(d18:0/16:0)	724.57	562.52	
HexCer(d18:1/h16:0)	738.56	576.51	
HexCer(d17:0/h17:0)	740.57	578.52	
HexCer(d18:0/h16:0)			
HexCer(d18:0/h17:0)	754.59	592.54	
HexCer(d18:1/h18:0)	766.59	604.54	
HexCer(d19:0/h17:0)	768.60	606.55	
HexCer(dX:Y/hZ:0)	$[M+Na]^+$	Fragment **c** $[M+Na - C_6H_{120}O_6]^+$	45
HexCer(d18:1/16:0)	722.56	542.49	
HexCer(d18:0/16:0)	724.57	544.50	
HexCer(d18:1/h16:0)	738.56	558.49	
HexCer(d17:0/h17:0)	740.57	560.50	
HexCer(d18:0/h16:0)			
HexCer(d18:0/h17:0)	754.59	574.52	
HexCer(d18:1/h18:0)	766.59	586.52	
HexCer(d19:0/h17:0)	768.60	588.53	

Compound	Precursor ion [m/z]	Product ion [m/z]	Collision energy [eV]
HexCer(dX:Y/hZ:0)	$[M+Na]^+$	Fragment **McL** $[M+Na - (FA\text{-}C_2H_4O_2)]^+$	45
HexCer(d18:1/16:0)	722.56	526.35	
HexCer(d18:0/16:0)	724.57	528.36	
HexCer(d18:1/h16:0)	738.56	526.35	
HexCer(d18:1/h18:0)	766.59		
HexCer(d17:0/h17:0)	740.57	514.34	
HexCer(d18:0/h16:0)	740.57	528.36	
HexCer(d18:0/h17:0)	754.59		
HexCer(d18:0/h18:0)	768.60		
HexCer(d18:0/h20:0)	796.63		
HexCer(d18:0/h22:0)	824.66		
HexCer(d18:0/h24:1)	850.67		
HexCer(d18:0/h24:0)	852.69		
HexCer(d19:0/h17:0)	768.60	542.40	
HexCer(dX:Y/hZ:0)	$[M+Na]^+$	Fragment **d** $[M+Na - (FA\text{-}H_2O)]^+$	45
HexCer(d18:1/16:0)	722.56	484.34	
HexCer(d18:0/16:0)	724.57	486.35	
HexCer(d18:1/h16:0)	738.56	484.34	
HexCer(d17:0/h17:0)	740.57	472.21	
HexCer(d18:0/h16:0)		486.35	
HexCer(d18:0/h17:0)	754.59		
HexCer(d18:1/h18:0)	766.59	484.34	
HexCer(d19:0/h17:0)	768.60	486.35	
Compound	**Precursor ion [m/z]**	**Product ion [m/z]**	**Collision energy [eV]**
HexCer(dX:Y/hZ:0)	$[M+Na]^+$	Fragment **e** $[M+Na - (FA\text{-}CH_2O_2)]^+$	45
HexCer(d18:1/16:0)	722.56	512.33	
HexCer(d18:0/16:0)	724.57	514.34	
HexCer(d18:1/h16:0)	738.56	512.33	

HexCer(d17:0/h17:0)	740.57	500.21	
HexCer(d18:0/h16:0)		514.34	
HexCer(d18:0/h17:0)	754.59		
HexCer(d18:1/h18:0)	766.59	512.33	
HexCer(d19:0/h17:0)	768.60	514.34	

Suppl. Table S5: Mass and mass error of GalCer$_{MLI}$ determined by high resolution-mass spectrometry

Sample	Sum Formula	Theoretical mass	Experimental mass	Mass error (Da)	Mass error (ppm)
	Precursor ion				
B. fragilis			740.56508	-0.00038	0.508
caecum			740.56458	0.00012	0.167
	$C_{40}H_{79}NO_9Na$	740.564704			
α GalCer(d18:0/βh16:0)			740.56484	0.-00014	0.184
β GalCer(d18:0/βh16:0)			740.56473	-0.00003	0.035
	Product ions				
	Fragment b				
B. fragilis			578.51210	-0.00022	0.380
caecum			578.51212	-0.00024	0.415
	$C_{34}H_{69}NO_4Na$	578.511880			
α GalCer(d18:0/βh16:0)			578.51196	-0.00008	0.138
β GalCer(d18:0/βh16:0)			578.51197	-0.00009	0.156
	McLafferty (McL)				
B. fragilis	$C_{25}H_{49}NO_8Na$	514.335038	514.33528	-0.00024	0.471
caecum			528.35097	-0.00028	0.534
α GalCer(d18:0/βh16:0)	$C_{26}H_{51}NO_8Na$	528.350688	528.35078	-0.00009	0.174
β GalCer(d18:0/βh16:0)			528.35078	-0.00009	0.174
	Fragment d				
B. fragilis	$C_{23}H_{47}NO_7Na$	472.32447	472.32476	-0.00029	0.614
Caecum			486.34035	-0.00023	0.473
	$C_{24}H_{49}NO_7Na$	486.34012			
α GalCer(d18:0/βh16:0)			486.34022	-0.00010	0.206

β GalCer(d18:0/βh16:0)			486.34022	-0.00010	0.206
	McL - Hexose				
B. fragilis	$C_{19}H_{37}NO_2Na$	334.271650	334.27197	-0.00032	0.957
Caecum			348.28759	-0.00029	0.833
α GalCer(d18:0/βh16:0)	$C_{20}H_{39}NO_2Na$	348.287300	348.28730	0	0
β GalCer(d18:0/βh16:0)			348.28743	-0.00013	0.373

Supplemental Figures

Suppl. Fig. 1

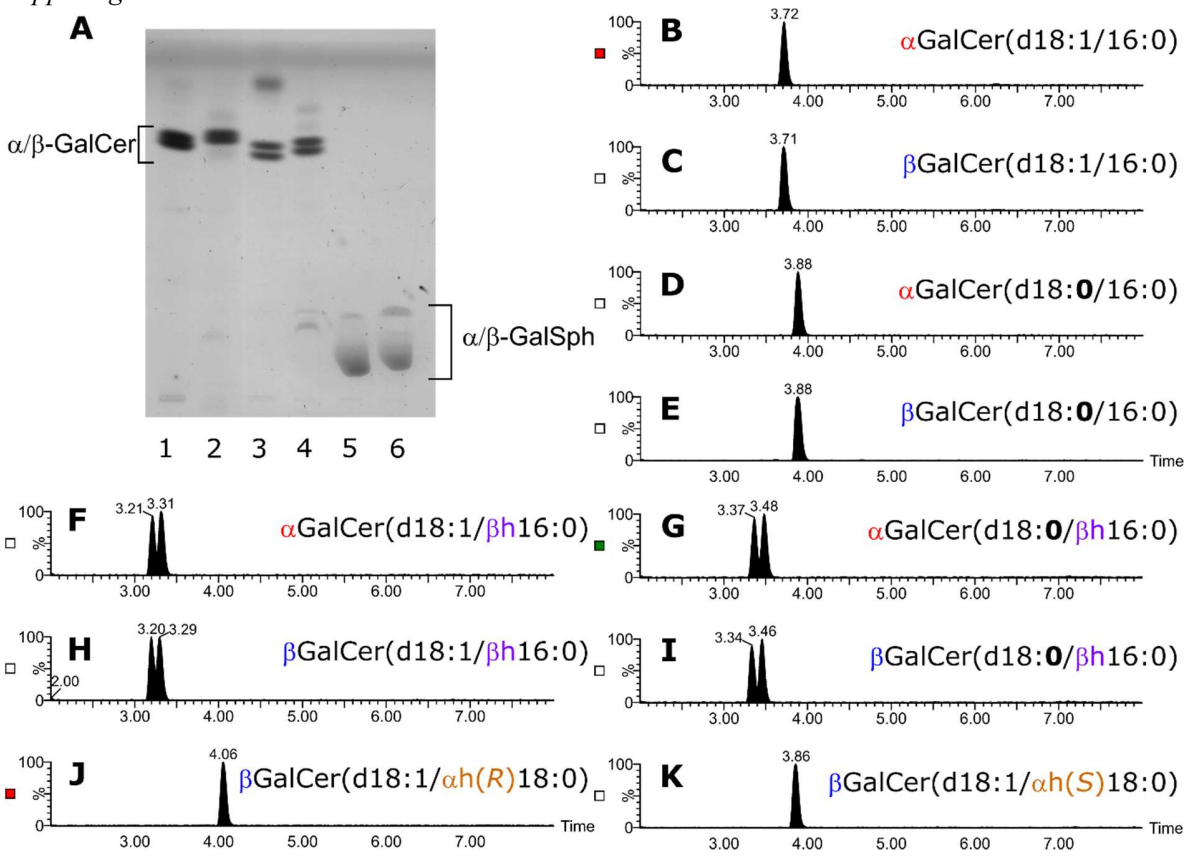

Legend to supplemental figure 1: Thin layer chromatography of synthetic B(d)S-GalCer (A) and total ion chromatograms of synthetic GalCers recorded by RP18-LC-MS^2 in product ion mode (B-K). The RP18-LC gradient contained 10 mM ammonium acetate as additive. A) Lane 1, BS-**α**GalCer(d18:1;h16:0), Lane 2, BdS-**α**GalCer(d18:0;h16:0), Lane 3, BS-**β**GalCer(d18:1;h16:0), Lane 4, BdS-**β**GalCer(d18:0;h16:0), Lane 5, **α**GalSph(d18:1), Lane 6, **β**GalSph(d18:1). B) NS-**α**GalCer(d18:1;16:0), C) NS-**β**GalCer(d18:1;16:0), D) NdS-**α**GalCer(d18:0;16:0), E) NdS-**β**GalCer(d18:0;16:0), F) BS-**α**GalCer(d18:1;h16:0), G) BdS-**α**GalCer(d18:0;h16:0), H) BS-**β**GalCer(d18:1;h16:0), I) BdS-**β**GalCer(d18:0;h16:0), J) AS-**β**GalCer(d18:1;3R-h18:0), and K) AS-**β**GalCer(d18:1;3S-h18:0). Note, AS-compounds elute approximately 0.49' (see Suppl. Fig. 5K and 5M) later due to increased acyl chain length. Taking this into account, B(d)S-GalCers elute on RP18 in front of A(d)S-GalCers followed finally by N(d)S-GalCers. Compounds with sphinganine (dS) elute later than compounds containing sphingosine (S).

Suppl. Fig. 2

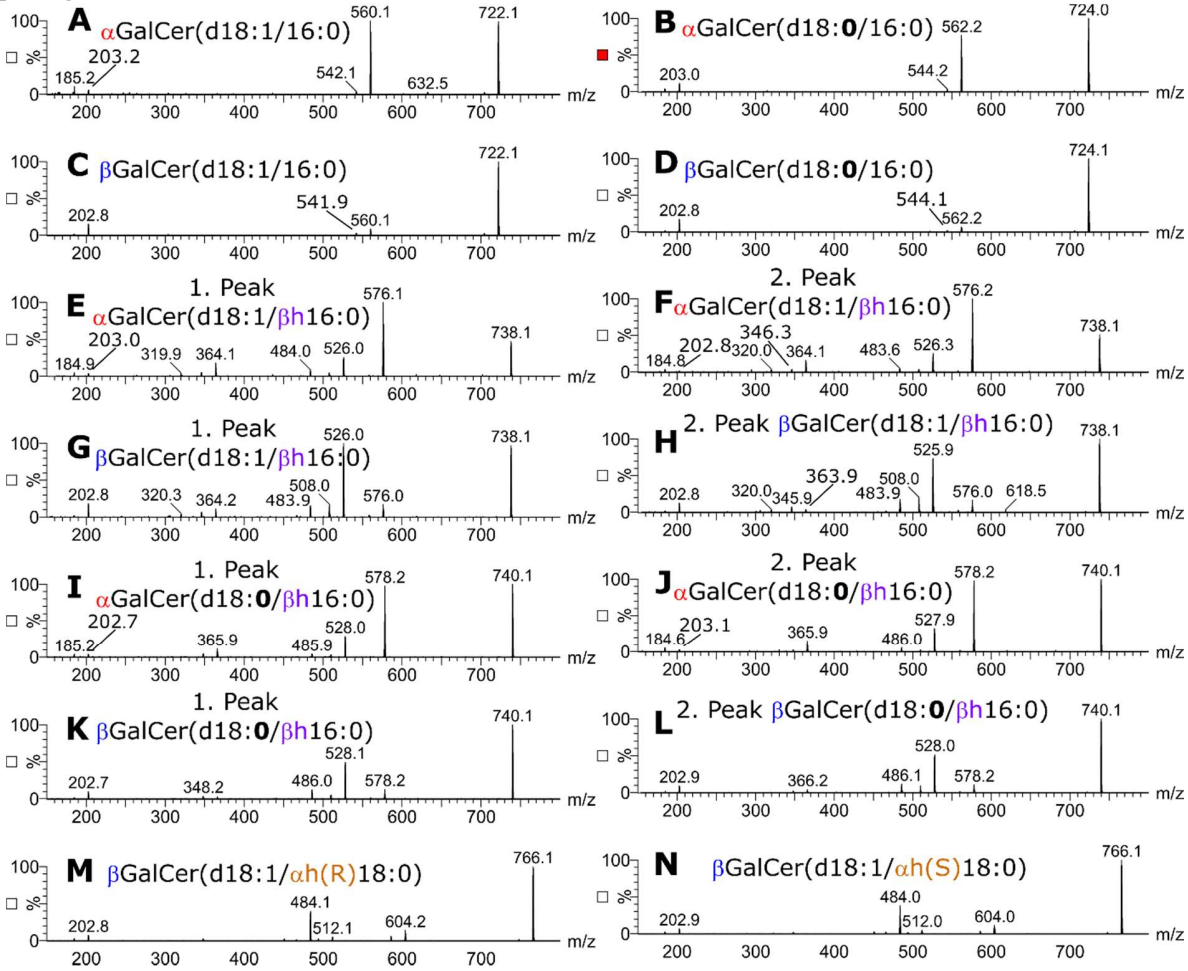

Legend to supplemental figure 2: Product ion spectra of sodium adducts of synthetic Galactosylceramides (GalCers). Product ion ion spectra induced by CID were recorded at 45V and obtained from the RP18-LC peaks shown in Suppl. Fig. 2. A) NS-**α**GalCer(d18:1;16:0), B) NdS-**α**GalCer(d18:0;16:0), C) NS-**β**GalCer(d18:1;16:0) D) NdS-**β**GalCer(d18:0;16:0), E) First peak of BS-**α**GalCer(d18:1;h16:0) eluting at 3.21', F) Second peak of BS-**α**GalCer(d18:1;h16:0) eluting at 3.31', G) First peak of BS-βGalCer(d18:1;h16:0) eluting at 3.20', H) Second peak of BS-**β**GalCer(d18:1;h16:0) eluting at 3.29', I) First peak of BdS-**α**GalCer(d18:0;h16:0) eluting at 3.37', J) Second peak of BdS-**α**GalCer(d18:0;h16:0) eluting at 3.48', K) First peak of BdS-**β**GalCer(d18:0;h16:0) eluting at 3.34', L) Second peak of BdS-**β**GalCer(d18:0;h16:0) eluting at 3.46', M) AS-**β**GalCer(d18:1;3R-h18:0), and N) AS-**β**GalCer(d18:1;3S-h18:0). Note, no difference between

the fragmentation pattern of the first and second peak of B(d)S-GalCers containing mixtures with 3R- and 3S-hydroxylated acyl chains. All 4 probes of B(d)S-GalCers show in addition to the McL-fragment (m/z 526 for BS and m/z 528 for BdS), but a fragment corresponding to the McL-fragment with additional loss of the sugar moiety (m/z 364 for BS and m/z 366 for BdS). The sodiated hexose ion (m/z 203) is recognized in all spectra.

Suppl. Fig. 3

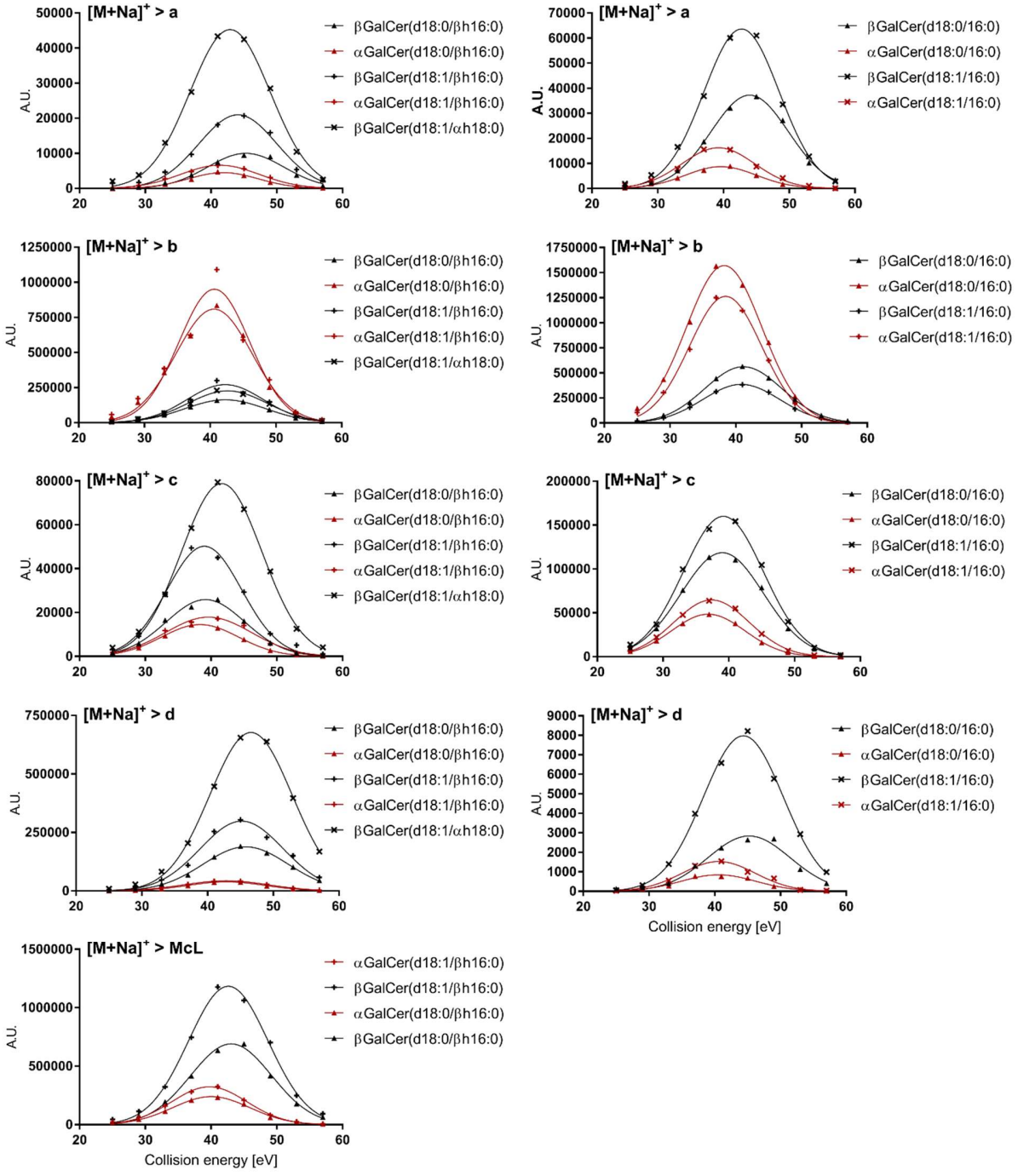

Legend to supplemental figure 3: Intensities of CID-fragments a, b, c, McL, and d arising from sodiated GalCer in dependence of the collision energy. N(d)S- and B(d)S-GalCers contain a C18-base and a C16:0 acyl chain. AS-GalCer contain a C18:0 acyl chain instead.

Suppl. Fig. 4

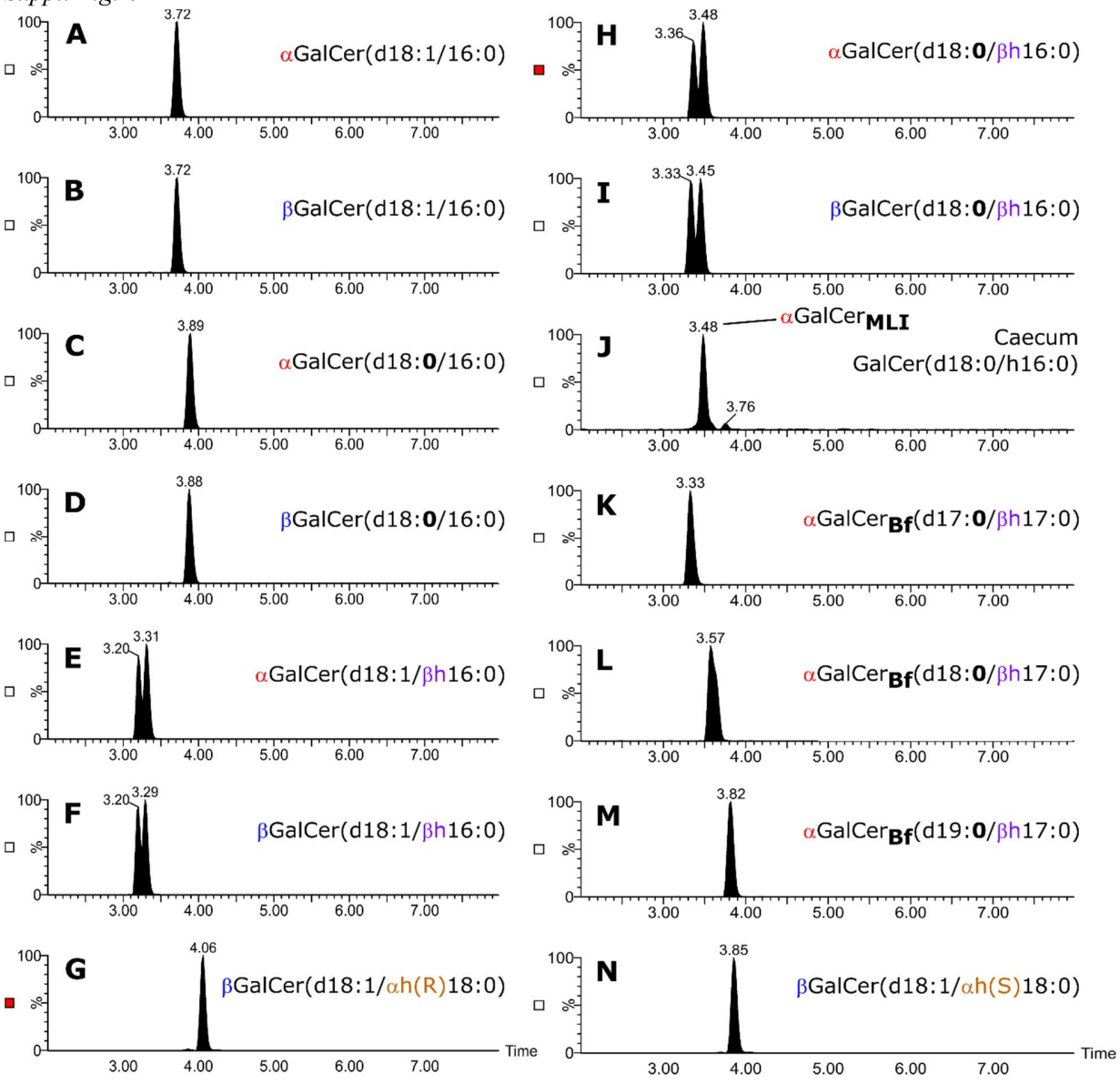

Legend to supplemental figure 4: Total ion chromatograms (TICs) of synthetic GalCers, BdS-**α**GalCers from B. fragilis and BdS-GalCer(d18:0;h16:0) enriched from mouse caecum recorded by RP18-LC-MS^2. The RP18-LC gradient contained 10 mM ammonium acetate as additive. TICs correspond to the transitions of the sodiated GalCer ions to the CID-fragments a, b, c, McL, d, and d' at 45V recorded in MRM mode. **A**) NS-**α**GalCer(d18:1;16:0), **B**) NS-**β**GalCer(d18:1;16:0), C**)** NdS-**α**GalCer(d18:0;16:0), **D**) NdS-**β**GalCer(d18:0;16:0), **E**) BS-**α**GalCer(d18:1;h16:0), **F**) BS-**β**GalCer(d18:1;h16:0), **G**) AS-**β**GalCer(d18:1;3R-h18:0), **H**), BdS-**α**GalCer(d18:0;h16:0) **I**) BdS-**β**GalCer(d18:0;h16:0), J) BdS-

GalCer(d18:0;h16:0) from mouse caecum, the peak at 3.48 min corresponds to **α**GalCer$_{\mathbf{MLI}}$, **K**) BdS-**α**GalCer(d17:0;h17:0) from B. fragilis, **L**) BdS-**α**GalCer(d18:0;h17:0), **M**) BdS-**α**GalCer(d19:0;h17:0) from B. fragilis, and N) AS-**β**GalCer(d18:1;3S-h18:0). Note, BdS-GalCer from Ceacum elutes like the second peak of synthetic BdS-**α**GalCer(d18:0;h16:0). AS-compounds elute approximately 0.49' (compare **K** and **M** to estimate shift by C_2H_4) later due to increased acyl chain length.

Suppl. Fig. 5

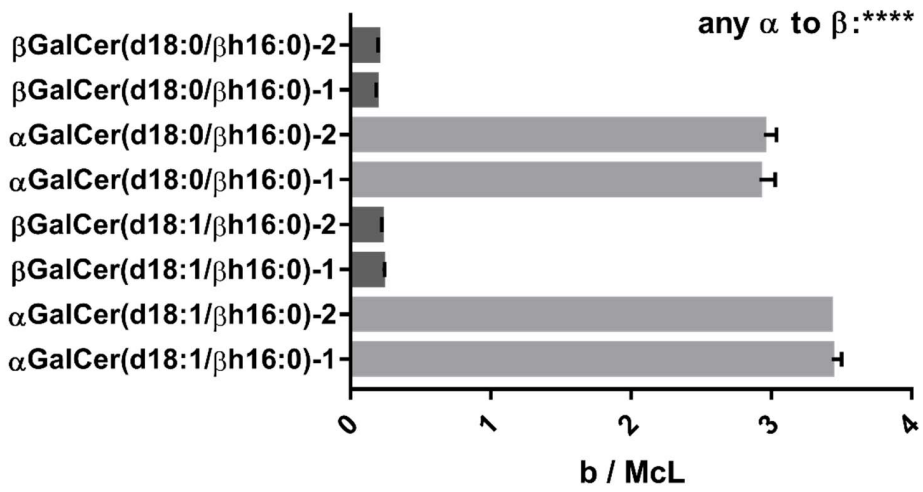

Legend to supplemental figure 5: Ratio of the intensities of MS^2-fragment b over the McL-fragment (see Fig. 2A and Suppl. Table S4) from synthetic B(d)S-GalCers with C18-base and hydroxylated C16:0-acyl chain after CID at 45V. In **α**-anomeric compounds McL is always weaker than fragment b, but in **β**-anomeric compounds it is vice versa. The b/McL-ratio differs significantly (****: $p < 0.0001$) between any **α**- and **β**-anomeric GalCer with a factor of **α**(b/McL) /**β**(b/McL) being 15.6 ± 0.7 for corresponding ceramide anchors. n = 3.

Suppl. Fig. 6

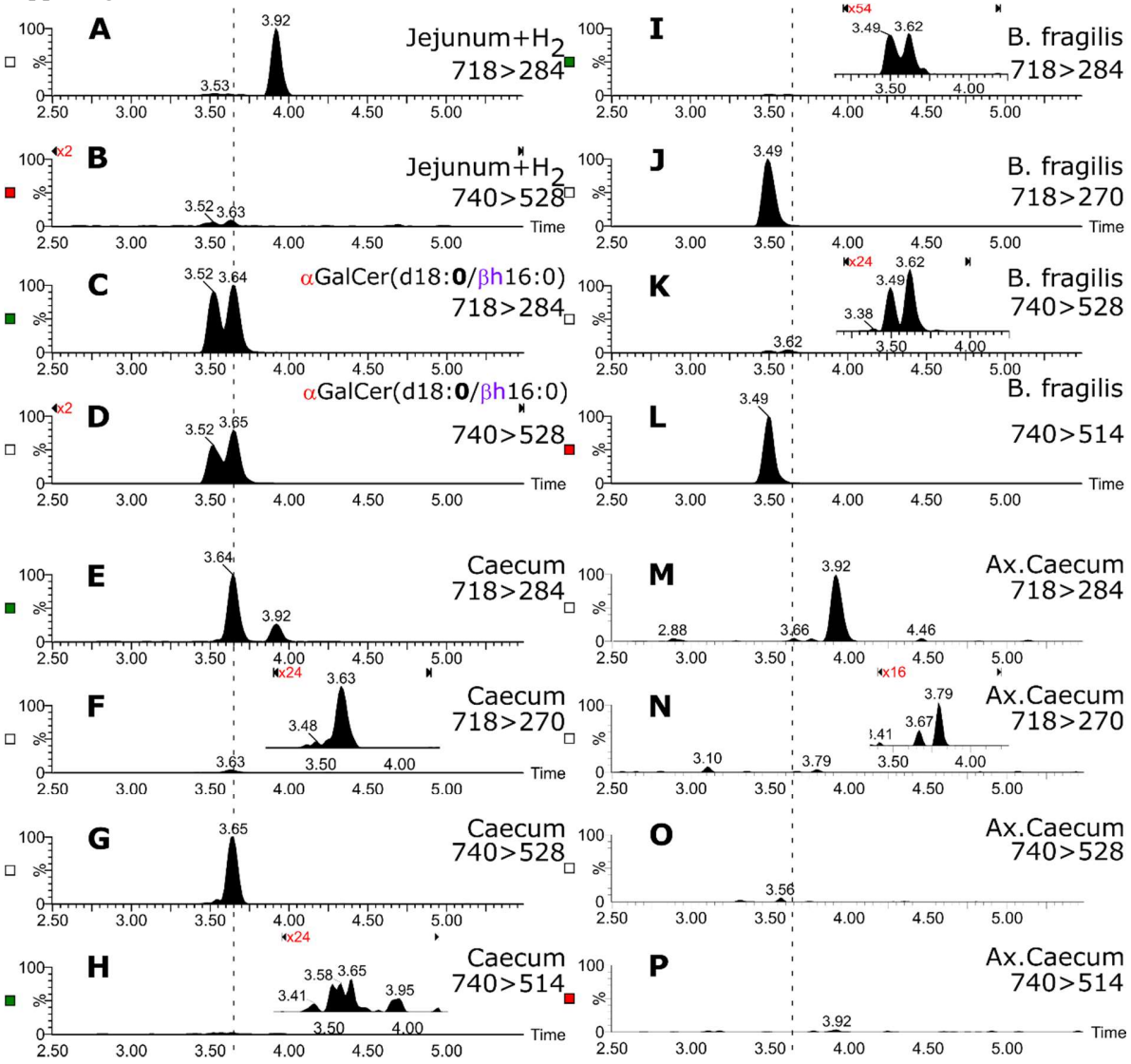

Legend to supplemental figure 6: RP18-LC-MS^2 showing extracted ion chromatograms (EICs) of synthetic GalCers, BdS-**α**GalCers from B. fragilis, BdS-GalCer(d18:0;h16:0) from caecum of normal and axenic mice, as well as AdS-**β**GlcCers derived from mouse jejunum extract after hydration. The RP18-LC gradient contained 10 mM ammonium formiate and 0.1% formic acid as additive. BdS-GalCer(d18:0;h16:0), i.e. **α**GalCer$_{MLI}$, from caecum of mice containing normal commensals (**E-H**) is recorded at a retention time of 3.64 ± 0.01 min with the transition $[M+H]^+ > [Sph\text{-}H_2O + H]^+$ (**E**) and $[M+Na]^+ > [McL]^+$ (**G**) eluting identical to the second peak of synthetic BdS-**α**GalCer(d18:0;h16:0) (**C** and **D**) recorded with the transition $[M+H]^+ > [Sph\text{-}H_2O + H]^+$ (**C**) and $[M+Na]^+ > [McL]^+$ (**D**). The minor

HexCer(d18:0;h16:0)-peak observed in normal ceacum (E) at 3.92’ elutes identical to AdS-**β**GlcCer(d18:1; h16:0) generated by hydration of a mouse jejunum extract (**A**). The latter does not reveal a corresponding McL-fragment at 3.92’ (**B**). A faint peak for BdS-GalCer(d17:0;h17:0) could be present in caecum at 3.65’ (**F** and **H**), similar, but not identical to the iso-branched BdS-**α**GalCer(d17:0;h17:0) present in B. fragilis (**J** and **L**). The latter could contain minor amounts of BdS-**α**GalCer(d18:0;h16:0) as indicated by the faint peaks at 3.49’ and 3.62’ (**I** and **K**). Extracts from caecum of axenic mice (**M**-**P**) do not reveal a peak for BdS-GalCer(d18:0;h16:0) at 3.64’ (**M** and **O**), and neither for BdS-GalCer(d17:0;h17:0) (**N** and **P**), but still contain the peak at 3.92’ correlating with AdS-βGlcCers derived from mouse jejunum extract after hydration (**M**). Normalization of intensities: B to A, D to C, F to E, H to G, I to J, K to L, and N, O, and P were normalized to M. The gradient used here, contained 10mM ammonium formiate and 0.1% formic acid (see Material and Methods).

Suppl. Fig. 7

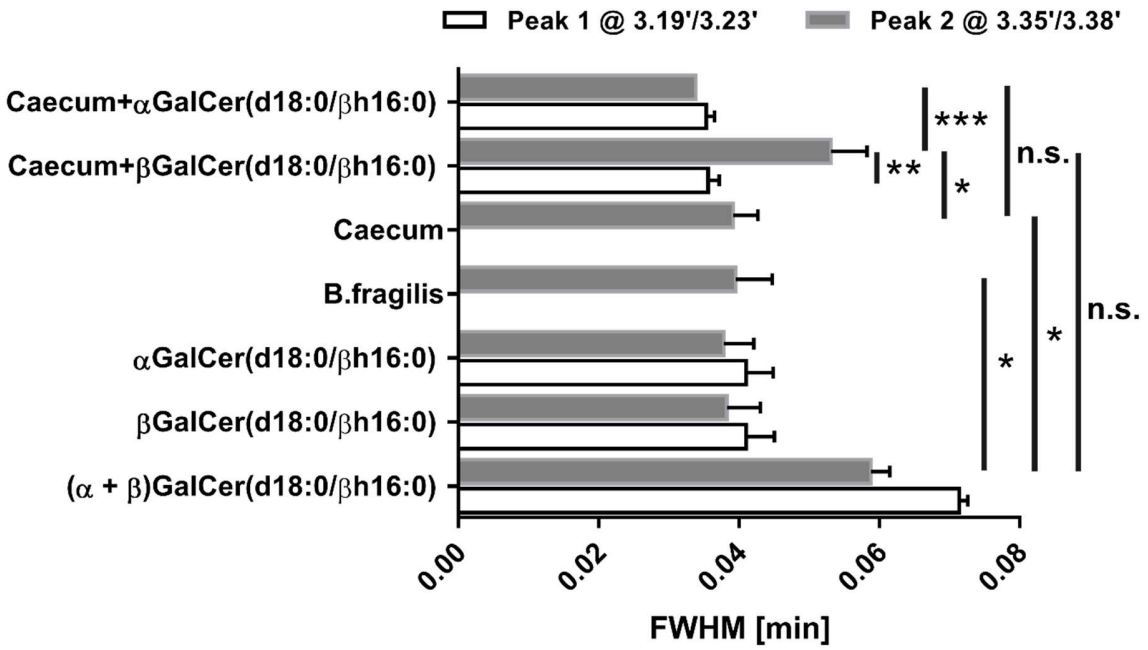

Legend to supplemental figure 7: Full Width at Half Height (FWHH) of BdS-GalCer peaks recorded by HILIC-MS^2. Note, mixing either synthetic BdS-**α**GalCer (BdS-**α**) with BdS-**β**GalCer (BdS-**β**) or Caecum **α**GalCer$_{\mathbf{MLI}}$ with synthetic BdS-βGalCer leads to significant peak broadening as determined at FWHH. This is not observed, when mixing Caecum **α**GalCer$_{\mathbf{MLI}}$ with synthetic BdS-**α**GalCer.

Suppl. Fig. 8

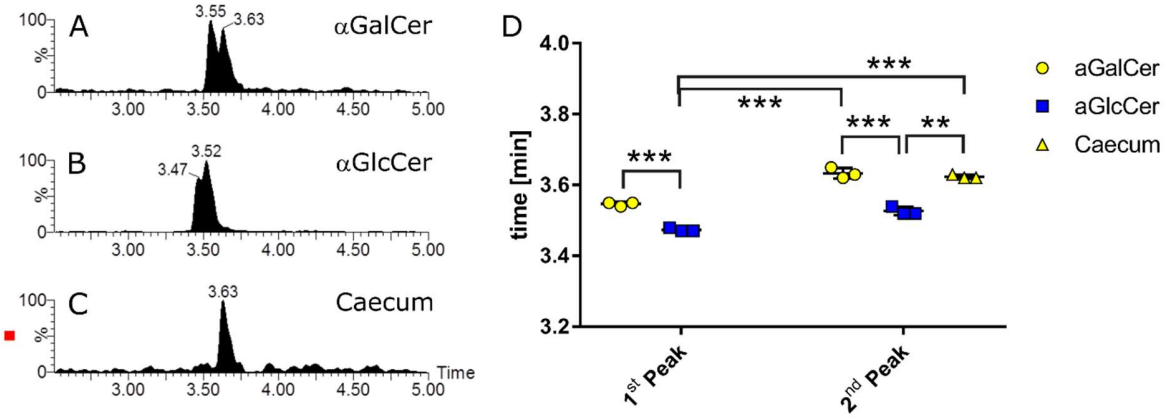

Legend to supplemental figure 8: Comparison of BdS-**α**GalCer, BdS-**α**GlcCer, and the corresponding BdS-**α**GalCer found in total caecum by HILIC-MS^2. Note that both peaks of **α**GlcCer elute significantly earlier than αGalCer and the corresponding **α**GalCer$_{\mathbf{MLI}}$ from total caecum.

Suppl. Fig. 9

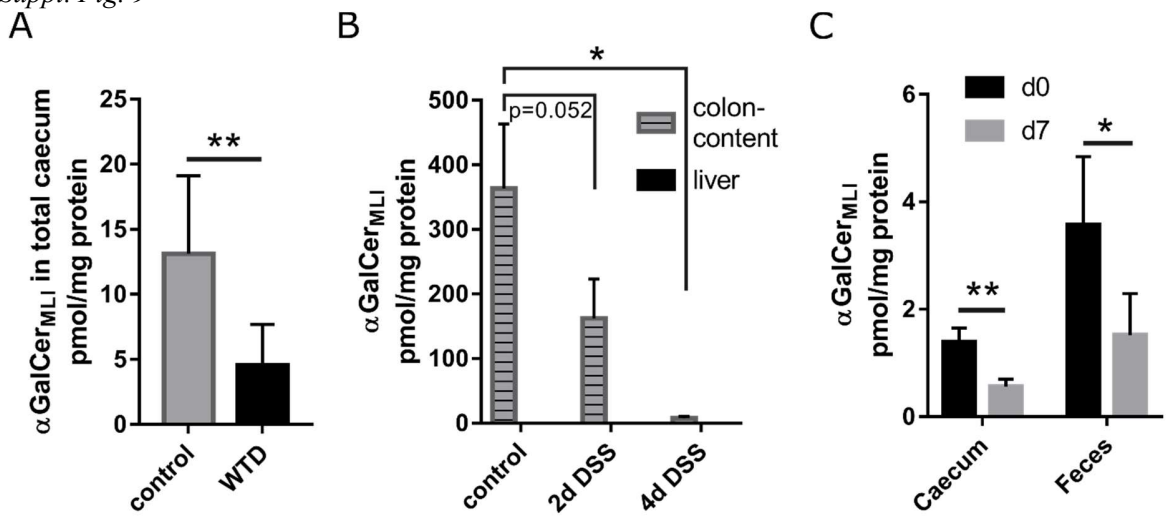

Legend to supplemental figure 9: Levels of large intestinal and fecal **α**GalCer$_{MLI}$ are influenced by diet (**A**), inflammation (**B**) and viral infection (**C**). **A)** Male C57Bl/6N mice (23-36 weeks old) were fed for 7 days control or Western type diet (WTD) and total caecum was analyzed for the presence of **α**GalCer$_{MLI}$. **B)** Male C57Bl/6 mice (9-11 weeks old) were treated with dextran sodium sulfate (DSS) to induce colitis. After corresponding time points, liver and content of colon was isolated and analyzed for **α**GalCer$_{MLI}$. **C)** Male C57BL/6 mice (8 weeks old) were infected with influence virus A. Total caecum and feces were analyzed at day zero (non-infected mice) and at day 7. Data of **A)** and **B)** were obtained with RP18-LC-MS^2 and Data of **C)** with HILIC-MS^2 method. WTD treated mice were C57Bl/6N from DKFZ SPF-animal facility, C57Bl/6 mice treated with DSS were from animal facility of EMBL, Heidelberg, and lung infection model was performed with C57BL/6J mice at the INSERM in Lille.

Suppl. Fig. 10

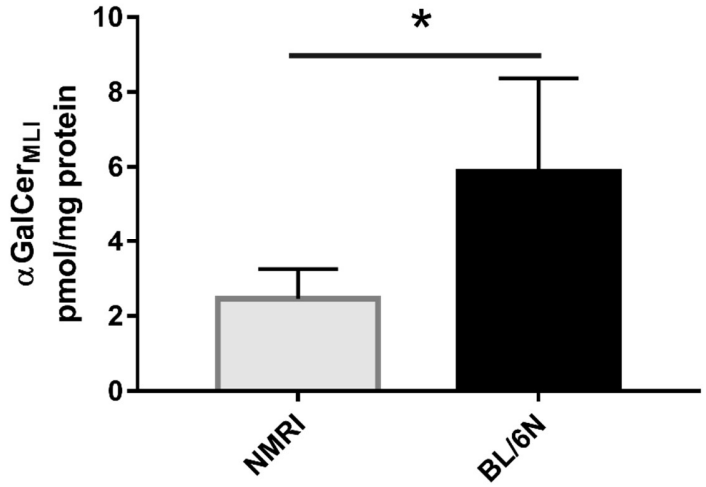

Legend to supplemental figure 10: Quantification of BdS-**α**GalCer(d18:0;h16:0) (**α**GalCer$_{\mathbf{MLI}}$) in total caecum of male mice obtained from Charles River, Sulzfeld. C57BL76N (BL/6N) mice contained 2.2fold more **α**GalCer than corresponding NMRI mice. For quantification the RP18-LC-MS^2 method was used.